Journal of Crystal Growth 477 (2017) 77–81

Contents lists available at ScienceDirect

Journal of Crystal Growth

journal homepage: www.elsevier.com/locate/crys

Growth rate dependence of boron incorporation into $B_xGa_{1-x}As$ layers

H. Detz [a,b,*], D. MacFarland [b], T. Zederbauer [b], S. Lancaster [b], A.M. Andrews [b], W. Schrenk [b], G. Strasser [b]

[a] Austrian Academy of Sciences, Dr. Ignaz Seipel-Platz 2, 1010 Wien, Austria
[b] Center for Micro- and Nanostructures and Institute for Solid-State Electronics, TU Wien, Floragasse 7, 1040 Wien, Austria

ARTICLE INFO

Article history:
Available online 27 February 2017
Communicated by Jean-Baptiste Rodriguez

Keywords:
A3. Molecular beam epitaxy
B1. Arsenides
B2. Semiconducting III-V materials
A1. High resolution X-ray diffraction
A1. Doping

ABSTRACT

This work provides a comprehensive study of the incorporation behavior of B in growing GaAs under molecular beam epitaxy conditions. Structural characterization of superlattices revealed a strong dependence of the BAs growth rate on the GaAs growth rate used. In general, higher GaAs growth rates lead to a higher apparent BAs growth rate, although lower B cell temperatures showed saturation behavior. Each B cell temperature requires a minimum GaAs growth rate for producing smooth films. The B incorporation into single thick layers was found to be reduced to 75–80% compared to superlattice structures. The p-type carrier densities in 1000 nm thick layers were found to be indirectly proportional to the B content. Furthermore, 500 nm thick $B_xGa_{1-x}As$ layers showed significantly lower carrier concentrations, indicating B segregation on the surface during growth of thicker layers.

1. Introduction

Boron-arsenide has not been characterized to the same detailed level as other binary III-V materials. Naturally, there are only sparse reports for the bowing parameters of the ternary alloy $B_xGa_{1-x}As$. This lack of data is mainly caused by difficulties in the epitaxy of BAs or $B_xGa_{1-x}As$ layers. The compositional range of $B_xGa_{1-x}As$ spans zincblende lattice parameters from 0.4777 nm to 0.56535 nm, devoid of suitable substrates for epitaxial growth. Furthermore, B does not only act as group III substitutional atom and form simple random alloys, as it is the case for $Al_xGa_{1-x}As$, $In_xGa_{1-x}As$ and $In_yAl_{1-y}As$. Antisite defects resulting in acceptor-like behavior were identified in several works for liquid-encapsulated Czochralski (LEC) growth and metal-organic chemical vapor deposition (MOCVD) [1–3]. B was found to segregate to the surface and crystallize in its subarsenide form $B_{12}As_2$ [3]. Finally, molecular beam epitaxy (MBE) growth studies on $B_xGa_{1-x}As$ are not common due to technical difficulties, as B requires either high-temperature effusion cells or electron-beam sources due to its low vapor pressure.

Despite these issues, $B_xGa_{1-x}As$ is an interesting candidate for strain-engineering in III-V heterostructures. Strain imposes limitations onto the maximum layer thickness and range of possible compositions for the pseudomorphic growth, e.g. of $In_xGa_{1-x}As$ on GaAs or InP. Already the addition of a minor fraction of B allows to balance or compensate compressive strain and therefore provides a greater flexibility in the material selection for multi-layer structures.

Earlier works on MBE-grown $B_xGa_{1-x}As$ agree on a decreasing incorporation for substrate temperatures above 550 °C [4,5]. The incorporation at higher temperatures could be recovered using Bi as a surfactant. Furthermore, B was found to act as p-type dopant in GaAs [6].

In order to integrate $B_xGa_{1-x}As$ into more complex structures, it is imperative to understand the incorporation of B, which is not as straightforward as it may seem. We provide a comprehensive study for the incorporation of B into $B_xGa_{1-x}As$ layers with respect to different GaAs growth rates. The corresponding samples are analyzed structurally by high-resolution X-ray diffraction (XRD), atomic force microscopy (AFM) and electronically via conductivity and Hall measurements.

2. Experimental procedure

The samples discussed in this work were grown on nominally on-axis GaAs (001) substrates by solid-source molecular beam epitaxy using a common substrate temperature of 600 °C and excess As_4 flux. Boron flux was supplied from a water-cooled high-temperature effusion cell, which was loaded with B powder (6 N) in a pyrolithic graphite crucible and operated in the range of 1725–1800 °C.[1] A visual inspection of the effusion cell after this

* Corresponding author at: Austrian Academy of Sciences, Dr. Ignaz Seipel-Platz 2, 1010 Wien, Austria.
E-mail address: hermann.detz@tuwien.ac.at (H. Detz).

[1] The charge material was obtained from Alfa Aesar, where Si, P, Fe, Zn and Fe were specified as main contaminants at the order of 0.5 ppm or lower.

http://dx.doi.org/10.1016/j.jcrysgro.2017.02.043
0022-0248/

study showed no visible charge depletion or corrosion of the crucible.

To study the incorporation of B under different conditions, the GaAs growth rate was varied within the range of 0.2–0.7 μm/h. Initial experiments regarding the incorporation of B were performed using GaAs/$B_xGa_{1-x}As$ superlattices, since they allow an increased total thickness due to strain energy reduction. Additionally, they provide more accurate compositional analysis using the separation between the 0th order diffraction and the substrate around the GaAs (0 0 4) diffraction, as well as the angular spacing of the fringe peaks. The superlattice period and the angular separation between the GaAs substrate and the 0th order superlattice peak serve as two independent results, which can be quantified. Assuming a general applicability of Vegard's law, this allows the fitting of two variables, which are the GaAs growth rate and an apparent BAs rate, respectively [7]. The superlattice structure consisted of ten periods of 14 nm GaAs and 30 nm $B_xGa_{1-x}As$. Furthermore, single thick $B_xGa_{1-x}As$ layers were prepared for electrical characterization and compared with superlattice samples grown under similar conditions.

All structures were analyzed by high-resolution XRD to determine the superlattice period and position of the 0th-order peak or the corresponding layer peak around the GaAs (0 0 4). The roughness of the topmost $B_xGa_{1-x}As$ layer of the superlattice samples was additionally characterized by AFM. Hall measurements were performed on single 500 or 1000 nm thick $B_xGa_{1-x}As$ layers, which were grown on semi-insulating GaAs (0 0 1) substrates, using a GaAs growth rate of 0.7 μm/h. Ohmic p-type contacts in the van-der-Pauw geometry were fabricated by thermal evaporation and a lift-off process using a sequence of 5 nm Au/10 nm Zn/100 nm Au.

3. Results and discussion

Structural characterization of the GaAs/$B_xGa_{1-x}As$ superlattices allow an estimation of the B content and provide a measure for the overall layer quality. Compositional analysis by XRD as well as surface morphology studies by AFM are discussed in Sections 3.1 and 3.2, respectively. The electronic properties due to unintentional doping as determined by Hall measurements are summarized in Section 3.3.

3.1. Apparent BAs growth rate

A series of superlattice samples with varying GaAs growth rates from 0.2–0.7 μm/h were analyzed by XRD for different B cell temperatures in the range of 1725–1800 °C. Representative $\omega - 2\theta$ scans around the GaAs (004) position for a B cell temperature of 1725 °C are plotted in Fig. 1. Except for the lowest GaAs growth rate, all scans show superlattice fringes and Pendellösung oscillations due to the total thickness of the structure.

Corresponding data for superlattices at different GaAs growth rates and B cell temperatures are summarized in Fig. 2. These data points would be expected to align along horizontal lines for each B cell temperature for a sticking and incorporation coefficient of unity. The fact that there is an obvious dependence on the GaAs growth rate implies that the incorporation of B at the growth surface is not trivial. Similar effects were also observed for MOCVD grown $B_xGa_{1-x}As$ layers [3].

The data points in Fig. 2 distinguish two qualitatively different situations. For effusion cell temperatures of $T \leqslant 1750$ °C, the data series shows an expressed kink around 0.4 μm/h. Lower GaAs growth rates also cause lower apparent BAs rates. Higher GaAs growth rates lead to a saturation of the observed BAs rate. In contrast, the highest B cell temperature of 1800 °C showed a linear

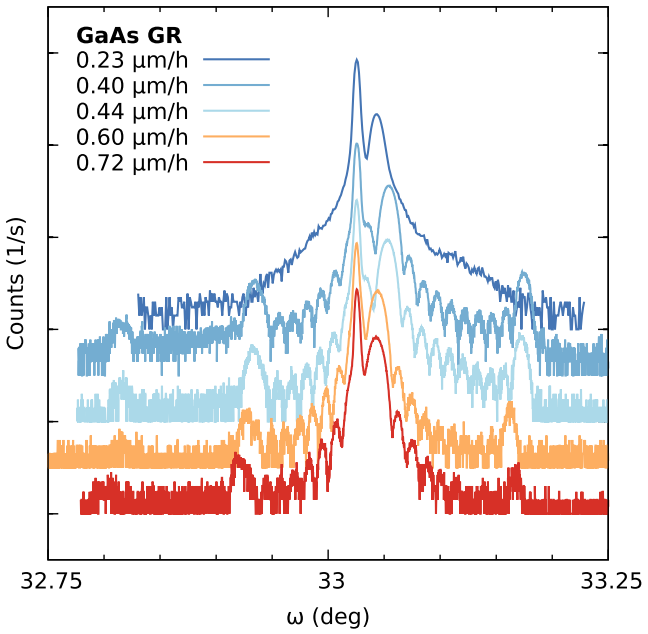

Fig. 1. High-resolution XRD scans of $B_xGa_{1-x}As$/GaAs superlattices around the GaAs (004) diffraction. The superlattices consisted of ten periods of 14 nm GaAs and 30 nm $B_xGa_{1-x}As$. The GaAs growth rate was varied between 0.23–0.72 μm/h at a constant B cell temperature of 1725 °C.

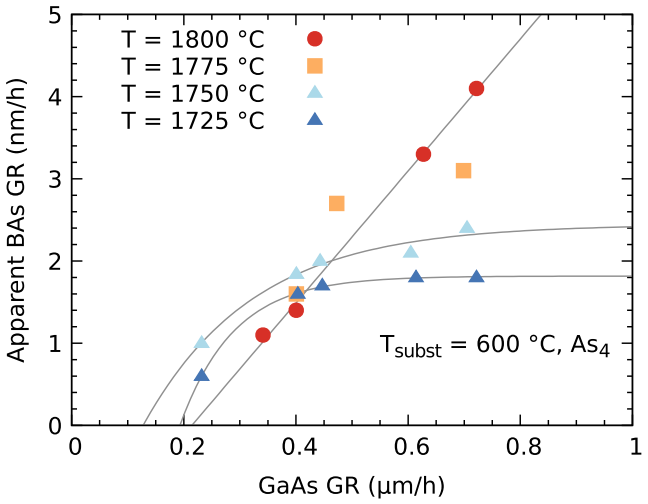

Fig. 2. Apparent BAs growth rates for different GaAs growth rates and B cell temperatures. While for B cell temperatures $T \leqslant 1750$ °C, the maximum achievable BAs rate settles. Higher B temperatures still allow a continuous increase.

relation between the GaAs and BAs growth rates. Possible saturation behavior beyond a GaAs rate of 0.7 μm/h can not be excluded, but this range is not accessible for technical limitations. A notable difference compared to the data series at lower B cell temperatures is the lower BAs growth rate, observed for GaAs rates ⩽0.4 μm/h. The data series for $T = 1775$ °C seem to be at the transition from one regime to the other. It should be noted that the direct relation between GaAs growth rate and B incorporation by keeping the As_4 flux constant and therefore effectively decreasing V/III ratio disagrees with earlier reports, which showed an increasing B content with higher V/III ratios [4].

Additionally, the incorporation behavior of B was studied for the case of thick layers. A comparison of the obtained apparent BAs growth rates in superlattice and single layer structures for

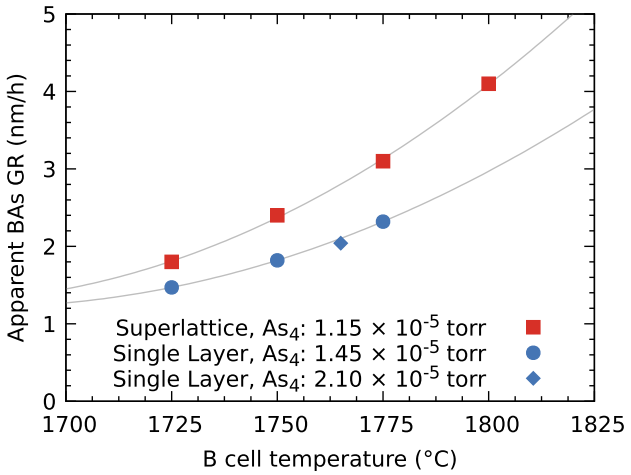

Fig. 3. Apparent BAs growth rates for GaAs/$B_xGa_{1-x}As$ superlattices and single $B_xGa_{1-x}As$ layers. In general, the B incorporation in thick layers is reduced to 75–80%, compared to the thin superlattice layers over the respective B cell temperature range. The single $B_xGa_{1-x}As$ layer, which was grown at a B cell temperature of 1765 °C and a higher As_4 flux of 2.1×10^{-5} torr, compared to 1.45×10^{-5} torr for the other samples, indicates that the incorporation behavior is independent of the III/V ratio used.

different B cell temperatures is plotted in Fig. 3. A reduced incorporation efficiency in the range of 75–80% is evident over the whole temperature range compared to the thin superlattice layers. One sample was grown at a higher As_4 flux (2.1×10^{-5} vs. 1.45×10^{-5} torr) but is still in-line with the fitted curve.

3.2. Surface roughness

The morphology of the topmost $B_xGa_{1-x}As$ layer of these superlattice samples was analyzed by AFM scans as another measure of material quality. Surface profiles of samples grown at different GaAs growth rates and B cell temperatures, including extracted RMS values, are shown in Fig. 4. It is evident that samples grown at lower GaAs rates show a strongly increased roughness with typical values in the range of 110–125 nm. In contrast, samples grown at higher GaAs rates resemble flat wafer surfaces with RMS values around 0.3–0.4 nm. Due to the large discrepancy in feature sizes, roughness analysis was performed on 5×5 μm scans for low growth rates and 1×1 μm scans for higher growth rates.

The observed RMS roughness shows a strong dependence on the GaAs growth rate, as plotted in Fig. 5. Each of the individual data series for different B cell temperatures shows a sharp drop over more than two orders of magnitude at a characteristic GaAs growth rate, which depends on the B cell temperature. The fact that a GaAs rate of 0.47 μm/h and a B temperature of 1775 °C leads to an intermediate roughness again suggests that this represents the transition between two incorporation regimes, as mentioned in section 3.1. RMS values of approximately 3.27 nm for a 1×1 μm^2 scan and 36.7 nm for a 5×5 μm^2 scan were obtained for this case.

3.3. Unintentional doping

The lower than expected B-content in both the superlattices and single layer samples, as discussed in Section 3.1, leads to the conclusion that some amount of the B atoms occupies B_{As} antisites and therefore acts as acceptors. The electronic carrier concentration was investigated for a set of unintentionally doped $B_xGa_{1-x}As$ layers with thicknesses of 500 and 1000 nm. All of these structures were grown at a GaAs rate of 0.7 μm/h to ensure a maximum incorporation of B. Carrier densities obtained from four-point conductivity and Hall measurements at room temperature are summarized in Fig. 6.

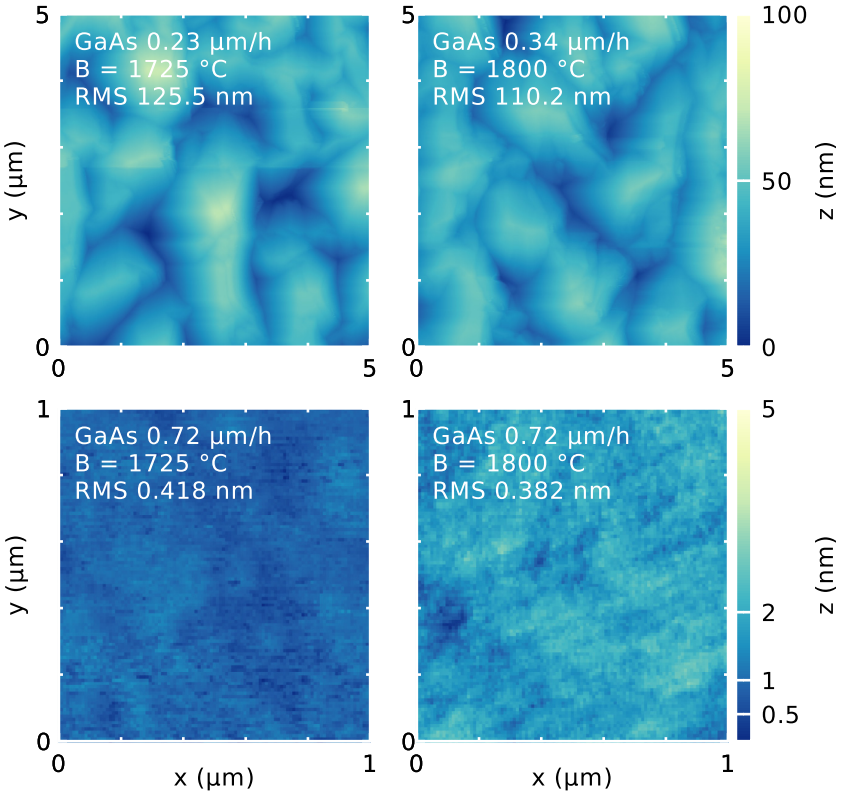

Fig. 4. Representative AFM images for low and high GaAs growth rates and B cell temperatures of 1725 and 1800 °C, respectively. While low GaAs growth rates lead to an RMS rougness exceeding 100 nm, high GaAs rates result in smooth surfaces and preserve the roughness of the initial substrates.

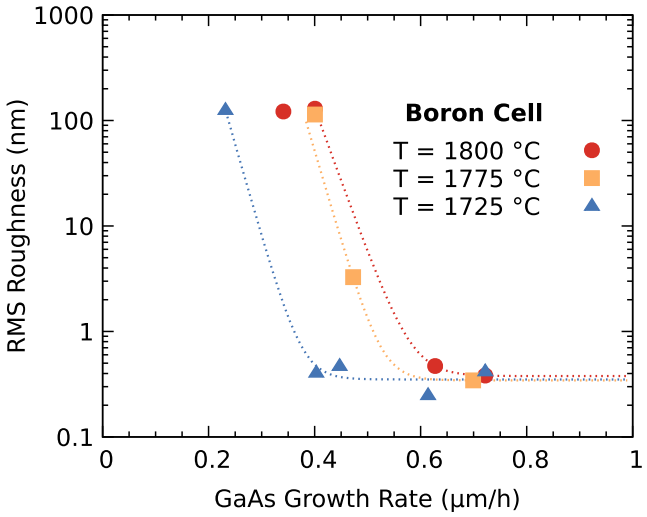

Fig. 5. RMS roughness of the topmost $B_xGa_{1-x}As$ superlattice layer for different GaAs growth rates and B cell temperatures. An increase in the GaAs growth rate clearly leads to a sharp drop in the measured surface roughness. The characteristic point shifts towards higher GaAs rates for increasing B cell temperatures.

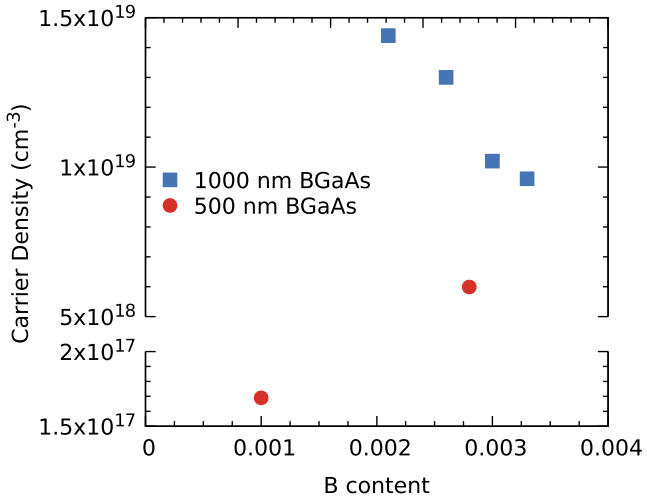

Fig. 6. P-type carrier concentration vs B content of single $B_xGa_{1-x}As$ layers with different thicknesses. Samples with a thickness of 1000 nm show a linear relation with a negative slope between B atoms acting as substitutionals and dopants, though with a doping efficiency around 10%. Thinner samples exhibit significantly lower carrier densities.

P-type carrier densities for 1000 nm thick layers exhibit a linear decrease with increasing B content. The absolute values in the range of 9×10^{18}–1.5×10^{19} cm^{-3} seem in good agreement with previous works [6,8]. However, there are some significant discrepancies. The relationship between substitutional B atoms and p-type carriers shows a negative linear slope. Every additional B_{Ga} atom corresponds to 0.1 less free charge carriers. While this appears in clear contrast to Ref. [8], it has to be pointed out that these data were obtained for lower B contents and potentially different growth rates and substrate temperatures, which are not reported in the referenced works.

Structures with a $B_xGa_{1-x}As$ layer thickness of 500 nm lead to clearly reduced carrier densities. Temperature-dependent measurements for these samples reveal an acceptor concentration of 1.69×10^{17}–5.99×10^{18} cm^{-3} at 300 K and a carrier freeze-out around 220 K. Corresponding data are compiled in Fig. 7. The lowest doping level was reached for a reduced As_4 flux of 8×10^{-6} torr

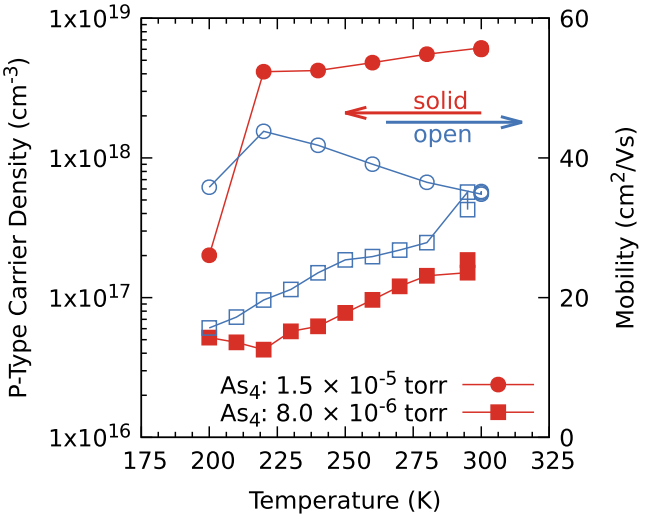

Fig. 7. Temperature dependence of carrier concentration and mobility for 500 nm thick $B_xGa_{1-x}As$ layers grown at a GaAs rate of 0.7 µm/h, a B cell temperature of 1800 °C and an As_4 flux of 8×10^{-6} and 1.5×10^{-5} torr. The sample grown at the lower As_4 flux showed a significantly lower p-type carrier density of 1.69×10^{17} cm^{-3}, compared to 5.99×10^{18} cm^{-3} for the sample grown at higher As_4 flux. The mobility values at room temperature are almost identical, yet show opposite behavior with respect to temperature.

during growth. These growth conditions are not fully characterized yet, but indicate an area of future research.

The carrier mobility for both 500 nm thick structures was found to be around 35 cm^2/Vs at 300 K. Compared to p-type GaAs with doping levels of 2×10^{17} and 6×10^{18} cm^{-3}, room temperature mobilities above 200 and 100 cm^2/Vs would be expected [9,10]. This deviation suggests that B atoms, in addition to isovalent substitution of Ga and B_{As} antisite behavior, are responsible for further scattering mechanisms, potentially due to charged defects or the formation of $B_{12}As_2$ clusters.

4. Summary

The incorporation of B into $B_xGa_{1-x}As$ layers under MBE growth conditions is shown to strongly depend on the GaAs growth rate. High-resolution XRD scans reveal different incorporation regimes. Low B cell temperatures ⩽1750 °C show a direct relation between the B incorporation and GaAs growth rate up to 0.4 µm/h, with saturation behavior above. The highest B cell temperature of 1800 °C leads to a linear relation between BAs and GaAs growth rates throughout the whole range studied. In contrast to superlattice structures, the B incorporation in single thick layers was found to be reduced to 75–80%. This deviation may be explained by surface segregation of B atoms during epitaxial growth.

Different incorporation regimes are corroborated by a surface roughness analysis using AFM scans. Samples grown at GaAs growth rates below 0.4 µm/h exhibit an RMS roughness of 110–125 nm, while samples at higher GaAs rates show flat surfaces with an RMS of 0.3–0.4 nm, independent of the B content.

Hall measurements for 1000 nm thick $B_xGa_{1-x}As$ layers revealed unintentional doping with hole conentrations in the range of 1×10^{19}–1.5×10^{19} cm^{-3}, which depend linearly on the B content in the layer. Thinner structures showed significantly lower carrier densities in the range of 1.69×10^{17}–5.99×10^{18} cm^{-3} with room-temperature mobilities around 35 cm^2/vs. The dependence on the layer thickness again indicates the potential formation of a different phase on the surface.

These findings allow a greater understanding of the B incorporation behavior and therefore enable the design of more complex structures using $B_xGa_{1-x}As$ layers for strain engineering.

Acknowledgments

H.D. is a recipient of an APART Fellowship of the Austrian Academy of Sciences. The authors acknowledge financial support by the Austrian Science Fund (FWF): P26100-N27 (H2N), as well as through the Gesellschaft für Mikro- und Nanoelektronik (GMe).

References

[1] L.B. Ta, H.M. Hobgood, R.N. Thomas, Evidence of the role of boron in undoped GaAs grown by liquid encapsulated Czochralski, Appl. Phys. Lett. 41 (11) (1982) 1091–1093, http://dx.doi.org/10.1063/1.93376.
[2] K. Elliott, Interaction between boron and intrinsic defects in GaAs, J. Appl. Phys. 55 (10) (1984) 3856–3858, http://dx.doi.org/10.1063/1.332896.
[3] H. Dumont, D. Rutzinger, C. Vincent, J. Dazord, Y. Monteil, F. Alexandre, J.L. Gentner, Surface segregation of boron in $B_xGa_{1-x}As$/GaAs epilayers studied by X-ray photoelecron spectroscopy and atomic force microscopy, Appl. Phys. Lett. 82 (12) (2003) 1830–1832, http://dx.doi.org/10.1063/1.1561164.
[4] M.E. Groenert, R. Averbeck, W. Hösler, M. Schuster, H. Riechert, Optimized growth of BGaAs by molecular beam epitaxy, J. Crystal Growth 264 (2004) 123–127, http://dx.doi.org/10.1016/j.jcrysgro.2004.01.010.
[5] A.J. Ptak, D.A. Beaton, A. Mascarenhas, Growth of BGaAs by molecular-beam epitaxy and the effects of a bismuth surfactant, J. Crystal Growth 351 (2012) 122–125, http://dx.doi.org/10.1016/j.jcrysgro.2012.04.026.
[6] W.E. Hoke, P.J. Lemonias, D.G. Weir, H.T. Hendriks, Molecular-beam epitaxial growth of boron-doped GaAs films, J. Vac. Sci. Technol. B 11 (1993) 902–904, http://dx.doi.org/10.1116/1.586734.
[7] A.R. Denton, N.W. Ashcroft, Vegard's law, Phys. Rev. A 43 (6) (1991) 3161–3164, http://dx.doi.org/10.11093/PhysRevA.43.3161.
[8] V.K. Gupta, M.W. Koch, N.J. Watkins, Y. Gao, G.W. Wicks, Molecular beam epitaxial growth of BGaAs ternary compounds, J. Electron. Mater. 29 (2000) 1387–1391, http://dx.doi.org/10.1007/s11664-000-0123-3.
[9] K. Saito, E. Tokumitsu, T. Akatsuka, M. Miyauchi, T. Yamada, M. Konagai, K. Takahashi, Characterization of p-type GaAs heavily doped with carbon grown by metalorganic molecular-beam epitaxy, J. Appl. Phys. 64 (8) (1988) 3975–3979, http://dx.doi.org/10.1063/1.341356.
[10] M. Wenzel, G. Irmer, J. Monecke, W. Siegel, Determination of the effective hall factor in p-type semiconductors, Semicond. Sci. Technol. 13 (5) (1998) 505–511, doi: 0268-1242/13/5/011.